Electron Pairing of Interfering Interface-Based Edge Modes

Sourav Biswas,* Hemanta Kumar Kundu,* Vladimir Umansky, and Moty Heiblum†
Braun Center for Submicron Research, Department of Condensed Matter Physics, Weizmann Institute of Science, Rehovot 7610001, Israel

(Received 11 April 2023; accepted 21 July 2023; published 1 September 2023)

The remarkable Cooper-like pairing phenomenon in the Aharonov-Bohm interference of a Fabry-Perot interferometer—operating in the integer quantum Hall regime—remains baffling. Here, we report the interference of paired electrons employing "interface edge modes." These modes are born at the interface between the bulk of the Fabry-Perot interferometer and an outer gated region tuned to a lower filling factor. Such a configuration allows toggling the spin and the orbital of the Landau level of the edge modes at the interface. We find that electron pairing occurs *only* when the two modes (the interfering outer and the first inner) belong to the *same* spinless Landau level.

DOI: 10.1103/PhysRevLett.131.096302

Despite extensive experimental and theoretical work since its discovery in the 1980s, the quantum Hall effect still provides a playground for extensive studies [1–5]. With an insulating bulk, transport studies are performed with the gapless edge modes. Because of "bulk-edge" correspondence, the nature of the bulk's quantum state is revealed [6–8]. Among the ubiquitous studies, the important ones are shot noise [9–11], interference and braiding [12–15], and thermal conductance measurements [16]. One of the intriguing and unexplained features is a pairing of electrons in bulk fillings $\nu_b > 2$. This phenomenon was observed in the interference of the outermost edge mode in a Fabry-Perot interferometer (FPI), with Aharonov-Bohm (AB) flux periodicity of $h/2e$, where e is the electron charge, and h is the Planck constant; suggesting interference of paired electrons ($e^* = 2e$) [17–20]. Efforts to understand fully this phenomenon failed thus far [21–23]. In order to understand the process leading to the pairing of electrons in a single edge mode, we utilize a new approach by interfering "interface edge modes" [24,25].

Normal edge modes are confined to the interface between the plane of the two-dimensional electron gas (2DEG) and the "vacuum." The transverse Hall conductance σ_{xy} is determined by the bulk filling ν_b: $\sigma_{xy} = (\nu_b e^2/h)$. Interface modes, on the contrary, are confined to the interface between two bulk regions with fillings: ν_b and ν_g (the latter is a gated bulk). Consequently, the transverse interface mode conductance is $\sigma_{xy} = (\nu_{int} e^2/h)$, with $\nu_{int} = (\nu_b - \nu_g)$, the interface filling. Recent charge and thermal transport measurements [25–28] reveal the potential of novel experiments employing 1D interface chiral modes. The schematic of the interface edge configuration, with $\nu_b = 2$ and $\nu_g = 1$, is shown in Fig. 1(a). At the interface, the counterpropagating modes "gap" each other as a result of full intermode charge equilibration, leaving the inner mode of $\nu_b = 2$ at the

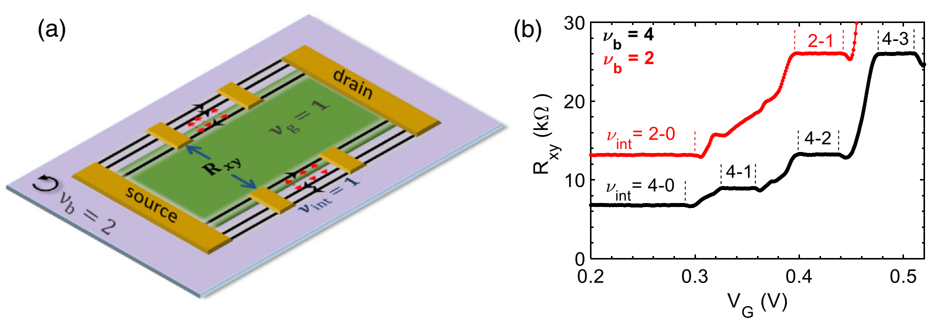

FIG. 1. Interface edge modes. (a) Schematic of interface edge modes. The bulk and gated region are shown in purple and green, respectively. The ohmic contacts (shown in yellow), made with Ni/Au/Ge evaporation followed by rapid thermal annealing, are placed at the interface. The gates are patterened by Pd/Au in cold evaporation. The bulk (gate) filling ν_b (ν_g) is tuned by the magnetic field (gate voltage V_G). When $\nu_b = 2$ and $\nu_g = 1$, full equilibration (shown by red arrows) between counterpropagating modes leads to one mode ($\nu_{int} = 1$) left at the interface. (b) Interface Hall resistance showing various integer plateaus with gate voltage V_G at the bulk filling $\nu_b = 2$ and 4. The bias cooling voltage for the gates is 0.55 V. The full depletion of the gate with filling underneath $\nu_g = 0$ starts at $V_G \approx 0.3$ V.

 © 2023 American Physical Society

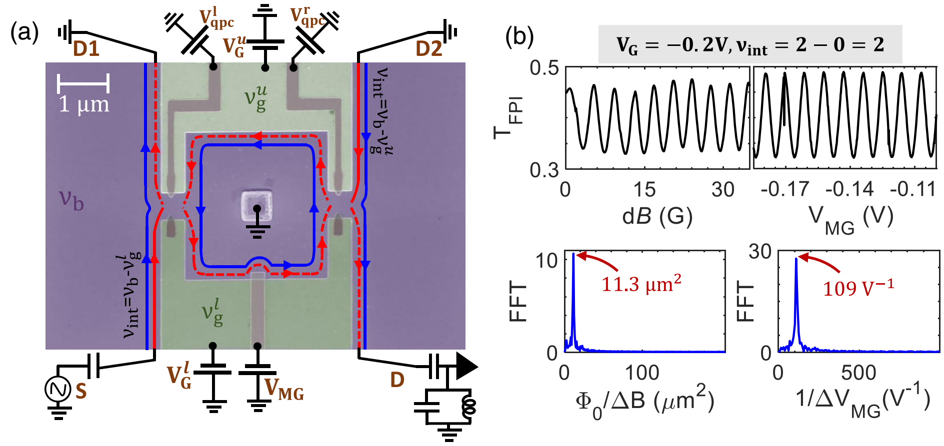

FIG. 2. Interface mode-based Fabry-Perot interferometer and Aharonov-Bohm oscillations. (a) False color scanning electron micrograph (SEM) image of the Fabry-Perot interferometer (FPI) with a grounded ohmic in the interior bulk. The lithographic internal area is 14.2 μm^2. The bulk region is shown in purple. The gates (shown in green) that form the interferometer are the narrow branches of two big gates—upper and lower gates—see Supplemental Material, Fig. S2 [29] for the full device structure. The ohmic contacts placed at the gate-bulk interface (see Fig. S2) measure the R_{xy} for the upper and lower interface modes. The depletion characteristics of the gates are identical, and the voltage $V_G^l = V_G^u = V_G$ tunes the filling underneath, hence the interface edge filling. The split gates as quantum point contacts, QPCs (brown) are separated from the lower gate (green) by 5 nm hafnium oxide. The incoming interface edge modes (ν_{int}) from the source (S) contact are biased with an ac voltage. The drain (D) contact measures the conductance as the transmission T_{FPI} through the FPI. The modulation gate (300 nm wide) sitting at the periphery of the interferometer tunes the area by V_{MG}. (b) Traces of T_{FPI} with magnetic field and modulation gate voltage showing AB oscillations when the outer edge at $2-0=2$ is weakly partitioned. The average transmission is $\overline{T_{FPI}} \approx 0.4$, and the individual QPC transmission (for the interfering outer edge) is $t \approx 0.89$. We assume the left and right QPC are identical with the transmission probability $t_{qpc}^l = t_{qpc}^r = t$, and thus the $\overline{T_{FPI}} = |t|^2$. The fast Fourier transformations (FFTs) with a single peak frequency are shown.

interface, with $\nu_{int} = 1$. Two examples of gate dependence of interface resistance with $\nu_b = 2$ and 4 are shown in Fig. 1(b).

It is worth recalling the main observations in the past "pairing experiments" [17,18] before we delve into new findings. Utilizing ubiquitous quantum Hall effect integer edge modes, we stumbled on electron pairing while interfering the outermost edge mode belonging to the first Landau level (LL), LL1↓, in bulk fillings exceeding $\nu_b = 3$, see Supplemental Material, Fig. S1 [29]. The interfering mode was accompanied by the first inner mode LL1↑ and the second inner mode LL2↓, both unpartitioned and encircling inside the interferometer (the arrow denotes the spin). Surprisingly, the first inner edge mode, LL1↑, was found to control the coherence and determine the flux periodicity of the interfering outermost edge mode. Moreover, the second inner mode, LL2↓, had to be populated to observe pairing.

Considering strong interedge interaction between the two outer edge modes at $2 < \nu < 3$, a flux periodicity of $\Phi_0/2$ and a (shot noise) Fano factor $F = 2$ clearly proves the pairing of electrons in the interfering (outermost) edge mode [21,22]. While the existing theory provides some suggestions, as we noted, it does not explain the many other observed effects such as the vital role of the inner mode.

Here, we replace the ubiquitous edge modes with interface modes, thus allowing controlling the character of the two outermost modes involved in the interference process. We test an AB FPI with bulk fillings, $2 \leq \nu_b \leq 6$, with different interface fillings determined by a neighboring gated bulk, thus adding crucial information essential to the underlying pairing mechanism [Fig. 3 and Table I].

The AB phase evolution is given by $\varphi_{AB} = (2\pi BA/\Phi_0)$, where B is the applied magnetic field, A is the area defined by the interfering edge mode, and $\Phi_0 = h/e$ the flux quantum [31,32]. With changing of the confined flux, the AB phase evolves as $\delta\varphi_{AB} = [2\pi(B\delta A + A\delta B)/\Phi_0]$, with the area changes by the modulation-gate voltage V_{MG}, with $\delta A = \alpha\delta V_{MG}$, and α is proportional to the gate-2DEG capacitance. Assuming first-order interference, i.e., weak backscattering by the two quantum point contacts (QPCs), the interference is proportionate to $\cos\delta\varphi_{AB}$. Customarily, a 2D *pyjama* plot [30,33,34] in the $B - V_{MG}$ plane leads to periodicities, $(1/\Delta B) = (A/\Phi_0)$ and $(1/\Delta V_{MG}) = (\alpha B/\Phi_0)$.

Our interface edge-based FPI [Fig. 2(a)], with an internal lithographic area of 14.2 μm^2, is fabricated in GaAs-AlGaAs heterostructure harboring high mobility 2DEG, with a 2D electron density of 1.7×10^{11} cm^{-2}, located 83 nm below the surface. Hafnium oxide isolates different metallic contacts. An interior small grounded ohmic contact reduces the charging energy of the FPI and enables AB interference. An ac voltage (1 μV at 900 kHz) is applied to the source, and the drain signal is amplified by a cold

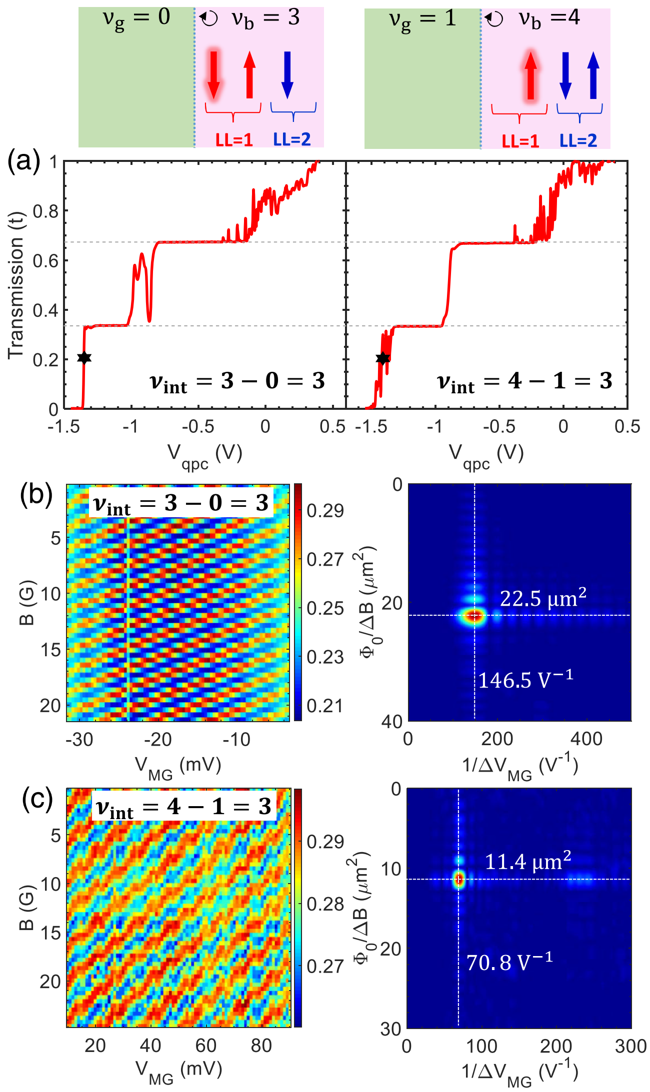

FIG. 3. Outer edge interference for two types of engineered $\nu_{\text{int}} = 3$, namely, $3 - 0 = 3$ and $4 - 1 = 3$. (a) The transmission (t) in the left quantum point contact (QPC) of the interferometer as a function of the QPC-gate-voltage V_{qpc} when the right QPC is fully open, showing three plateaus for both conditions for $\nu_{\text{int}} = 3$. Almost identical transmission is measured in the right QPC when the left one is open. The star symbol represents a typical partitioning of the outer mode for interference. The schematics on top represent the spin states (not to be confused with the chirality) of the edge modes (after full equilibration) that propagate for $3 - 0$ and $4 - 1$ edge configurations. The glowing one corresponds to the interfering (outer) edge. (b) The characteristic Aharonov-Bohm (AB) pyjama for $3 - 0$ (left) when the QPCs are set at $t \approx 88\%$ and the average transmission is $\overline{T_{\text{FPI}}} \approx 0.254$. The corresponding fast Fourier transformation (FFT) with frequency values is shown on the right. (c) The AB pyjama and the FFT for $4 - 1$, when the QPC transmission is $t \approx 92\%$, and $\overline{T_{\text{FPI}}} \approx 0.28$. The values of $(\Phi_0/\Delta B)$ and $(1/\Delta V_{\text{MG}})$ clearly show the interference of paired electrons ($2e$) at $3 - 0 = 3$, while the pairing is *not* observed at $4 - 1 = 3$. The comparisons are made with $2 - 0 = 2$ outer edge, see also Table I.

(1.5 K) amplifier (with an LC circuit at its input), cascaded by a room-temperature amplifier. Measurements are performed at 10 mK base temperature.

We first repeat the "pairing experiments" with trivial edge modes. Starting at $\nu_{\text{int}} = \nu_{\text{b}} - \nu_{\text{g}} = 2 - 0 = 2$, the FPI's QPCs are tuned to partition the outermost edge mode and fully reflect the inner mode [Fig. 2(a)]. High visibility conductance oscillations with magnetic field and modulation gate voltage, characteristics of an FPI in a coherent AB regime, are observed [Fig. 2(b)]. The obtained periodicities in B and V_{MG} correspond to an area $(\Phi_0/\Delta B) = 11.3\ \mu\text{m}^2$ and $(1/\Delta V_{\text{MG}}) = 109\ \text{V}^{-1}$, respectively. These data ensure electron interference ($e^* = e$) with the flux quantum periodicity. The smaller AB area than the lithographic one indicates ≈200 nm depletion at the gate interface.

Interfering the outermost mode at the $\nu_{\text{int}} = 3 - 0 = 3$ configuration [see Fig. 3(a), and see Supplemental Material, Fig. S4 [29] for a detailed schematic] with QPCs' transmission $t \approx 0.88$ leads to frequencies $(\Phi_0/\Delta B) = 22.5\ \mu\text{m}^2$ and $(1/\Delta V_{\text{MG}}) = 146.5\ \text{V}^{-1}$ [Fig. 3(b)]; namely, $h/2e$ flux periodicity and thus an apparent interfering charge $e^* = 2e$. As observed before [17], the filling of LL2↓ (second inner mode) is necessary to observe pairing in the interfering (outermost) mode in LL1↓.

To test the relation between the two outer modes, we toggled the interface mode's LL (spin and orbital) by tuning the ν_{b} and ν_{g}; here, $\nu_{\text{int}} = 4 - 1 = 3$ [Fig. 3(a)] with LL1↓ gapped out. The interfering outermost mode belongs to the spin-split Landau level LL1↑ (with $t \approx 0.92$), and adjacent, the enclosed first inner, belongs to the orbital LL2↓. Note that a "protective mode" the second inner mode, belonging to the LL2↑ Landau level, circulates inside the FPI. The observed periodicities, $(\Phi_0/\Delta B) = 11.4\ \mu\text{m}^2$ and $(1/\Delta V_{\text{MG}}) = 70.8\ \text{V}^{-1}$ [Fig. 3(c)], are similar to those of $2 - 0$ configuration, namely, no pairing. See Supplemental Material, Fig. S5 [29] for data with a strongly pinched QPC.

What is the main difference between the $3 - 0$ and $4 - 1$ configurations? In the $3 - 0$ case, the outermost interfering mode and the first inner mode belong to the same spinless Landau level, LL1, i.e., they share the same orbital (but carry opposite spins). In the $4 - 1$ case, though the pairs are spinless, the interfering mode belongs to LL1, while the first inner mode belongs to LL2. As seen above, pairing occurs when the two outer modes belong to the same spinless Landau level. Indeed, pairing is also observed in the $5 - 2$ configuration; i.e., the outermost mode belongs to LL2↓, the first inner mode belongs to LL2↑, and the protective mode is LL3↓ (see Supplemental Material, Fig. S6 [29]).

To further confirm the robustness and universality of the above pairing, we interfere various modes (inner and outer) at the bulk fillings $4 \leq \nu_{\text{b}} \leq 6$ (Supplemental Material, Figs. S7 and S8 [29]). The obtained results are tabulated in Table I. The different realizations allow a clear view of the needed conditions to observe pairing.

TABLE I. Summary of the results for different interference configurations. Obtained frequency values (in B and V_{MG} dependent oscillation traces, pyjamas), the estimated interfering charge (e^*), and the flux-periodicity ($\Delta\Phi$) for the interfering edge mode at interface filling $\nu_{\mathrm{int}} = \nu_{\mathrm{b}} - \nu_{\mathrm{g}}$. The modes (spin states) are shown by arrows with the first one starting from the left being outer (nearest to the bulk-gate interface) and the next ones being first inner, second inner, and so on. The interfering one is shown by the dashed arrow. The AB flux periodicity is obtained by comparing the field periodicities ΔB between filling factors and $\nu_{\mathrm{int}} = 2 - 0$ outer edge. The less area $(\Phi_0/\Delta B)$ for an inner edge is attributed to the presence of two more edge channels from the boundary. The interfering charge e^* at $B = B_2$ is estimated using gate voltage periodicities ΔV_{MG} and the relation $(e^*/e) = (B_1 \Delta V_{\mathrm{MG1}}/B_2 \Delta V_{\mathrm{MG2}})$ with $e^* = e$ (e.g., at $2 - 0 = 2$ outer edge) at $B = B_1$ [13,14]. Note that the equation assumes the mutual capacitance α between the interfering edge channel and modulation gate to be constant. However, α varies with the number of fully transmitted edge channels [30]. Therefore, the comparison of an inner mode with the outer one using this relation is not ideal and provides quite a large error in the value of e^*.

B (Tesla)	Interference configuration	$(\Phi_0/\Delta B)$ (μm^2)	$(1/\Delta V_{\mathrm{MG}})$ (V^{-1})	Flux periodicity	Interfering charge (e^*)	Paring
3.7	$2 - 0 = 2$ ⇣↑ (outer)	11.3	109	Φ_0	e	No
2.45	$3 - 0 = 3$ ⇣↑↓ (outer)	22.5	146.5	$\cong(\Phi_0/2)$	$\cong 2.03e$	Yes
1.85	$4 - 1 = 3$ ⇡↓↑ (outer)	11.4	70.8	$\cong\Phi_0$	$\cong 1.3e$	No
1.45	$5 - 2 = 3$ ⇣↑↓ (outer)	19	104	$\cong(\Phi_0/2)$	$\cong 2.4e$	Yes
1.85	$4 - 0 = 4$ ↓↑⇣↑ (second inner)	7.5	64.77	$\cong\Phi_0$	$\cong 1.18e$	No
1.45	$5 - 0 = 5$ ↑↓⇣↑↓ (second inner)	12.4	118	$\cong(\Phi_0/2)$	$\cong 2.7e$	Yes
1.22	$6 - 0 = 6$ ↓↑⇣↑↓↑ (second inner)	19	87	$\cong(\Phi_0/2)$	$\cong 2.4e$	Yes
1.22	$6 - 2 = 4$ ⇣↑↓↑ (outer)	21	86	$\cong(\Phi_0/2)$	$\cong 2.4e$	Yes

The exact mechanism of such intriguing paired electrons' interference is still not understood. Our new observations indicate that the interaction of the spin-split edge modes belonging to a single Landau orbital fundamentally differs from that in different Landau orbitals. In the former case, the spin up-down (↑↓) electrons seem to possess a low energy bosoniclike (zero-spin) state when the other interaction (edge bulk) is insignificant due to a protective inner mode. In another geometry, where a grounded drain is connected to the interfering mode, as in a Mach-Zehnder interferometer [17,18], the pairing effect is absent.

Aharonov-Bohm interference of paired electrons in integer quantum Hall remains a puzzling observation without an explanation. Together with past data, our new results, based on interfering interface edge mode, show the following. (a) Pairing occurs between modes belonging to the same spinful Landau level, hence, the pairs are spinless. (b) The paired modes must be accompanied by an inner mode (belonging to a higher Landau level). This mode does not affect the pairing but seems to protect (screen) the paired modes from the bulk. We did not observe yet such an effect in the fractional regime.

We thank D. E. Feldman for the useful discussion. We acknowledge the continuous support of the Sub-Micron Center staff. M. H. acknowledges the support of the European Research Council under the European Union's Horizon 2020 research and innovation program (Grant Agreement No. 833078), and the partial support of the Minerva Foundation with funding from the Federal German Ministry for Education and Research, under Grant No. 713534.

*S. B. and H. K. K. contributed equally to this work.
†Corresponding author: moty.heiblum@weizmann.ac.il

[1] K. von Klitzing, T. Chakraborty, P. Kim, V. Madhavan, X. Dai, and J. McIver, 40 years of the quantum Hall effect, Nat. Rev. Phys. **2**, 397 (2020).
[2] B. I. Halperin and J. K. Jain, *Fractional Quantum Hall Effects: New Developments* (World Scientific, Singapore, 2020).
[3] M. Z. Hasan and C. L. Kane, Colloquium: Topological insulators, Rev. Mod. Phys. **82**, 3045 (2010).
[4] S. D. Sarma and A. Pinczuk, *Perspective in Quantum Hall Effects* (Wiley, New York, 1996).
[5] R. Prange and S. M. Girvin, *The Quantum Hall Effect* (Springer Verlag, Berlin, 1990).
[6] B. I. Halperin, Quantized Hall conductance, current-carrying edge states, and the existence of extended states in a two-dimensional disordered potential, Phys. Rev. B **25**, 2185 (1982).
[7] X. G. Wen, Gapless boundary excitations in the quantum Hall states and in the chiral spin states, Phys. Rev. B **43**, 11025 (1991).

[8] M. Heiblum and D. E. Feldman, Edge probes of topological order, Int. J. Mod. Phys. A **35**, 2030009 (2020).

[9] R. dePicciotto, M. Reznikov, M. Heiblum, V. Umansky, G. Bunin, and D. Mahalu, Direct observation of a fractional charge, Nature (London) **389**, 162 (1997).

[10] L. Saminadayar, D. C. Glattli, Y. Jin, and B. Etienne, Observation of the $e/3$ Fractionally Charged Laughlin Quasiparticle, Phys. Rev. Lett. **79**, 2526 (1997).

[11] M. Heiblum, Quantum shot noise in edge channels, Phys. Status Solidi B **243**, 3604 (2006).

[12] Y. Ji, Y. Chung, D. Sprinzak, M. Heiblum, D. Mahalu, and H. Shtrikman, An electronic Mach-Zehnder interferometer, Nature (London) **422**, 415 (2003).

[13] J. Nakamura, S. Liang, G. C. Gardner, and M. J. Manfra, Direct observation of anyonic braiding statistics, Nat. Phys. **16**, 931 (2020).

[14] H. K. Kundu, S. Biswas, N. Ofek, V. Y. Umansky, and M. Heiblum, Anyonic interference and braiding phase in a Mach-Zehnder Interferometer, Nat. Phys. **19**, 515 (2023).

[15] H. Bartolomei *et al.*, Fractional statistics in anyon collisions, Science **368**, 173 (2020).

[16] M. Banerjee, M. Heiblum, V. Umansky, D. E. Feldman, Y. Oreg, and A. Stern, Observation of half-integer thermal Hall conductance, Nature (London) **559**, 205 (2018).

[17] H. K. Choi, I. Sivan, A. Rosenblatt, M. Heiblum, V. Umansky, and D. Mahalu, Robust electron pairing in the integer quantum Hall effect regime, Nat. Commun. **6**, 7435 (2015).

[18] I. Sivan, R. Bhattacharyya, H. K. Choi, M. Heiblum, D. E. Feldman, D. Mahalu, and V. Umansky, Interaction-induced interference in the integer quantum Hall effect, Phys. Rev. B **97**, 125405 (2018).

[19] J. Nakamura, S. Fallahi, H. Sahasrabudhe, R. Rahman, S. Liang, G. C. Gardner, and M. J. Manfra, Aharonov-Bohm interference of fractional quantum Hall edge modes, Nat. Phys. **15**, 563 (2019).

[20] A. Demir, N. Staley, S. Aronson, S. Tomarken, K. West, K. Baldwin, L. Pfeiffer, and R. Ashoori, Correlated Double-Electron Additions at the Edge of a Two-Dimensional Electronic System, Phys. Rev. Lett. **126**, 256802 (2021).

[21] G. A. Frigeri and B. Rosenow, Electron pairing in the quantum Hall regime due to neutralon exchange, Phys. Rev. Res. **2**, 043396 (2020).

[22] G. A. Frigeri, D. D. Scherer, and B. Rosenow, Sub-periods and apparent pairing in integer quantum Hall interferometers, Europhys. Lett. **126**, 67007 (2019).

[23] D. Ferraro and E. Sukhorukov, Interaction effects in a multichannel Fabry-Perot interferometer in the Aharonov-Bohm regime, SciPost Phys. **3**, 014 (2017).

[24] B. Dutta, W. Yang, R. Melcer, H. K. Kundu, M. Heiblum, V. Umansky, Y. Oreg, A. Stern, and D. Mross, Distinguishing between non-Abelian topological orders in a quantum Hall system, Science **375**, 193 (2022).

[25] S. Biswas, R. Bhattacharyya, H. K. Kundu, A. Das, M. Heiblum, V. Y. Umansky, M. Goldstein, and Y. Gefen, Shot noise does not always provide the quasiparticle charge, Nat. Phys. **18**, 1476 (2022).

[26] B. Dutta, V. Umansky, M. Banerjee, and M. Heiblum, Isolated ballistic non-Abelian interface channel, Science **377**, 1198 (2022).

[27] M. Yutushui, A. Stern, and D. F. Mross, Identifying the $\nu = 5/2$ Topological Order through Charge Transport Measurements, Phys. Rev. Lett. **128**, 016401 (2022).

[28] C. Lin, M. Hashisaka, T. Akiho, K. Muraki, and T. Fujisawa, Time-resolved investigation of plasmon mode along interface channels in integer and fractional quantum Hall regimes, Phys. Rev. B **104**, 125304 (2021).

[29] See Supplemental Material at http://link.aps.org/supplemental/10.1103/PhysRevLett.131.096302 for detailed device structure, edge schematics for various interference configurations, and additional data.

[30] N. Ofek, A. Bid, M. Heiblum, A. Stern, V. Umansky, and D. Mahalu, Role of interactions in an electronic Fabry-Perot interferometer operating in the quantum Hall effect regime, Proc. Natl. Acad. Sci. U.S.A. **107**, 5276 (2010).

[31] B. I. Halperin, A. Stern, I. Neder, and B. Rosenow, Theory of the Fabry-Perot quantum Hall interferometer, Phys. Rev. B **83**, 155440 (2011).

[32] B. Rosenow and B. I. Halperin, Influence of Interactions on Flux and Back-Gate Period of Quantum Hall Interferometers, Phys. Rev. Lett. **98**, 106801 (2007).

[33] Y. M. Zhang, D. T. McClure, E. M. Levenson-Falk, C. M. Marcus, L. N. Pfeiffer, and K. W. West, Distinct signatures for Coulomb blockade and Aharonov-Bohm interference in electronic Fabry-Perot interferometers, Phys. Rev. B **79**, 241304(R) (2009).

[34] I. Sivan, H. K. Choi, J. Park, A. Rosenblatt, Y. Gefen, D. Mahalu, and V. Umansky, Observation of interaction-induced modulations of a quantum Hall liquid's area, Nat. Commun. **7**, 12184 (2016).